MESHLESS 2D DIRECT NUMERICAL SIMULATION AND HEAT TRANSFER IN A BACKWARD-FACING STEP WITH HEAT CONDUCTION IN THE STEP

ANDRÉS G. VIDAL[1], ALAIN J. KASSAB[2], EDUARDO A. DIVO[3,4]

[1] Department of Mechanical, Materials and Aerospace Engineering
University of Central Florida
Orlando, FL 32816, United States
e-mail: Andres.Vidal@knights.ucf.edu

[2] Department of Mechanical, Materials and Aerospace Engineering
University of Central Florida
Orlando, FL 32816, United States
e-mail: Alain.Kassab@ucf.edu

[3] Department of Mechanical Engineering
Embry-Riddle Aeronautical University
Daytona Beach, FL 32114, United States

[4] Department of Mechanical, Materials and Aerospace Engineering
University of Central Florida
Orlando, FL 32816, United States
e-mail:edivo@mail.ucf.edu

Key words: Meshless Methods, Computing Methods, Direct Numerical Simulation, Heat Transfer.

Abstract. A meshless direct pressure-velocity coupling procedure is presented to perform Direct Numerical Simulations (DNS) and Large Eddy Simulations (LES) of turbulent incompressible flows in regular and irregular geometries. The proposed method is a combination of several efficient techniques found in different Computational Fluid Dynamic (CFD) procedures. With this new procedure, preliminary calculations with 2D steady state flows show that viscous effects become negligible faster that ever predicted numerically. The fundamental idea of this method lays on several important inconsistencies found in three of the most popular techniques used in CFD, segregated procedures, as well as in other formulations. The inconsistencies found become important in elliptic flows and they might lead to some wrong solutions. Preliminary calculations done in 2D laminar flows, suggest that the numerical diffusion and interpolation error are much important at low speeds, mainly when both, viscous and inertia forces are present. With this competitive and efficient procedure, the solution of the 2D Direct Numerical Simulation of turbulent flow with heat transfer on a backward-facing step is presented. The thermal energy is going to be transferred to the fluid through conduction on the step, with both constant temperature and heat flux conditions in the back wall of the step. The variation of the local Nusselt Number through the

wall will be studied and its corresponding effect in the energy transfer to the fluid.

1 INTRODUCTION

Since the introduction of the *Projection Method* by Harlow and Welch [1], the science of Computational Fluid Dynamics (CFD) has become a fundamental tool for engineering calculations and design. Basically, the velocity-pressure coupling is done in a segregated way, one equation at a time. After the publication of this procedure, almost all numerical methods developed in Computational Fluid Dynamics (CFD), with some minor modifications, the original flow equations are transformed into a series of consecutive and explicit equations for velocity, pressure and mass correction, this last one needed to satisfy the mass balance.

For highly demanding problems such as Direct Numerical Simulation (DNS) and Large-Eddy Simulation (LES), the normal approach is to extend the current CFD procedures and perform some minor changes intended to reduce the so-called *numerical diffusion error*. Once again, almost all procedures transform the original flow equations into a system of segregated equations.

In spite of the improvement in all CFD techniques, even today the solution of complex elliptic problems, such as the backward-facing step or lid-driven cavity is still a mayor challenge. These two cases have produced by far the largest amount of differences in numerical results between procedures. Many authors have explained this effect as *bifurcation of the solution*. The idea of this work is to present a meshless localized RBF procedure to solve the flow equations in the original form, so that there is no simplification or approximation of any boundary condition. The velocity-pressure coupling procedure is the same one developed in [2]. The staggered point distribution approach (or grid) is selected and the RBF scheme is chosen to perform any necessary interpolation. Finally, in order to keep the numerical diffusion at a very low level, the well known flux-limiting scheme will be used in the discretization of the convection term.

2 PREVIOUS WORK

In recent years, several studies have been performed where the influence of geometry and/or flow conditions on the heat transfer are analyzed. For example, in [3], a LES simulation is performed to study the heat transfer and fluid flow of a turbulent separating flow past a backward-facing step. A fully collocated grid is used and compressible flow is assumed at low Mach numbers. The bottom wall downstream of the step was supplied with a uniform heat flux and different heat flux levels were analyzed. Dramatic variation of the wall temperatures in the recirculation zone was observed with a steep increment in wall temperature close to the step followed by a decrease in the convective heat transfer. Another conclusion is that the viscous sub-layer played a critical role in controlling the heat transfer rate. The Reynolds analogy was not valid in the recirculation region.

On the other hand, in [4], simulations of turbulent flow adjacent a 2D backward-facing step are presented to explore the effects of step height on separation and heat transfer. The stepped wall is kept at a constant heat flux and the Reynolds number is fixed at 28,000. The remaining walls are isolated. Here, a two-equation low-Reynolds model is employed. The primary and secondary recirculation regions increase in size as the step size increases. The bulk temperature increases more rapidly as the step height increases. Additionally, increasing the step height causes the magnitude maximum kinetic energy to increase.

An interesting study can be seen in [5, 6], where a simulation is presented for a backward-facing step flow and heat transfer inside a channel with ribs turbulators. The problem was investigated for Reynolds numbers up to 32000. The effect of a step height, the number of ribs and the rib thickness on the flow and thermal field were investigated. The effect of turbulence was modeled by using a k-ϵ model with its wall function formulas. The obtained results show that the strength and size of the recirculation zones behind the step are increased with the increase of contraction ratio (i.e. with the in-crease of a step height). The size of recirculation regions and the reattachment length after the ribs are decreased with increasing of the contraction ratio.

In other works, such as [7], the effect on a pulsating flow and an oscillating wall is studied with a possible application in chamber combustors. Results of steady state and transient calculations are presented as well as the evaluation of several turbulence models. It was observed that the variations in the excitation frequency of the inlet flow and wall vibrations have an influence on the instantaneous heat transfer coefficient profile. However, significant effect on the time mean value and position of the heat transfer peak is only visible for the inlet velocity profile fluctuations with frequency approximately equal to the turbulence bursting frequency.

In [8], a numerical study is presented where a locally turbulent oscillating jet is used to evaluate the separation and reattachment. A three-equation turbulence model is used and different forcing frequencies were evaluated. A constant heat flux was imposed in the bottom wall. The time dependent distributions of the stresses indicated that heat transfer is significantly enhanced at the most effective frequency.

An experimental study can be found in [9], in which the backward-facing step is controlled by equipping a slit at the bottom cornet of the step. It was found that the heat transfer and pressure drop characteristics are controlled by the flow ratio. When the suction flow was 0.6, the highest performance was obtained.

Finally, in [10], the effect of a baffle in the entrance of the expansion is analyzed. Comparing the results with and without the baffle, its presence improves the average Nusselt number to a maximum of 190% for the heating step and 150% for the heating section. Additionally, a slight movement of the baffle can cause a drastic change in the flow structure and temperature distributions.

3 VELOCITY-PRESSURE COUPLING

The finite volume method proposed by Patankar [11], with SIMPLE and SIMPLER techniques as velocity-pressure coupling procedures, is the most popular method in CFD. These coupling schemes are used in most commercial and noncommercial CFD packages, using finite volume, finite difference or finite element method as the main discretization procedures.

However, these coupling procedures are known to produce significant numerical diffusion. The most general procedure (SIMPLER) can be resumed as:

1. Discretize momentum equation ($\hat{p} = p/\rho - \vec{r}\cdot\vec{g}$):

$$\vec{\hat{v}}_P = \frac{1}{a_P}\sum a_{nb}\vec{v}_{nb}\ ,\quad \vec{v}_P = -\vec{\hat{v}}_P + \frac{1}{a_P}\nabla\hat{p} \tag{1}$$

2. Compute pressure by introducing Eq. (1) into continuity equation:

$$\nabla\cdot\left(\frac{1}{a_P}\nabla\hat{p}\right) = \nabla\cdot\vec{\hat{v}}_P \tag{2}$$

3. Update pressure in Eq. (1) and solve for velocity.
4. Correct velocity to enforce mass continuity:

$$\vec{v} = \vec{v}^* + \vec{v}'\ ,\quad \hat{p} = \hat{p}^* + \hat{p}' \tag{3}$$

$$\nabla\cdot\left(\frac{1}{a_P}\nabla\hat{p}'\right) = -\nabla\cdot\vec{v}^* + \nabla\cdot\vec{\hat{v}}' \tag{4}$$

where the term $\nabla\cdot\vec{\hat{v}}'$ is frequently neglected. The first comment that it is convenient to make to this procedure is that, the main coefficient a_P is inside all partial derivatives in pressure and mass-correction equations. The structure of this coefficient is:

$$a_P = \nu C_L - u_P C_{DX} - v_P C_{DY} \tag{5}$$

with C_L, C_{DX} and C_{DY} the coefficients of the discretization scheme. For a non uniform mesh, the coefficient a_P is a function of the position. This coefficient will produce clearly numerical diffusion in Eqs. (1) and (2).

The only way that Eqs. (14) and (16) will not produce numerical diffusion is with a mesh of constant spacing and using central differencing in convection terms. Since a_P gathers the diffusion and convection terms, central differencing for convection derivative will not have any coefficient. With a uniform mesh, the diffusion term of $\vec{\hat{v}}$ is zero and the Eq. (4) becomes exactly the same projection procedure of Harlow and Welch [1].

By updating velocity in SIMPLER, the procedure becomes the same algorithm [1], but in SIMPLE, updating pressure with p' is updating pressure with the velocity potential. This explains why SIMPLE takes so many iterations to converge and why this procedure works only when velocity is corrected and not pressure (as initially inferred).

Another problem that SIMPLE and SIMPLER have is, in pressure equation (4), boundary conditions (pressure coefficient zero in all boundaries) imply that the viscosity of the fluid is infinite at the wall, inflows and outflows. The condition of viscosity infinite is correct at the wall but, at inflows and outflows is evidently incorrect. At inflows, this ***numerical change*** in the viscosity of the fluid produces a force that helps the motion of the fluid but, at outflows, this change in viscosity produces a force that decelerates the fluid. This is one reason why pressure equation (4) has problems converging, unless a block-correction or multigrid algorithm is used.

A useful alternative that solves the problems associated to both segregated and direct full coupling procedures is presented in [12]. In general, this scheme uses the segregated grid arrangement in the same way as finite volume method.

The fundamental aspect of this coupling approach is that the velocity-pressure coupling is done with the momentum and continuity equations in the original form. After substituting finite differencing expressions for both, viscous and convection terms, as well as the pressure gradient, the momentum and continuity equations can be written in the form:

$$\begin{gathered} a_P^u u_P + C_P^u \left(p_P - p_E\right) = b_P^u \\ a_P^v v_P + C_P^v \left(p_P - p_N\right) = b_P^v \\ D_P^u \left(u_P - u_W\right) + D_P^v \left(v_P - v_S\right) = 0 \end{gathered} \tag{6}$$

In the system (6), pressure and velocity components are located at different points, as expected in a staggered point distribution. The coupling of u, v and p is performed by writing, in all possible ways, a linear system of 3 equations of the kind:

$$\begin{pmatrix} a_{11} & 0 & a_{13} \\ 0 & a_{22} & a_{23} \\ a_{31} & a_{32} & 0 \end{pmatrix} \begin{pmatrix} u \\ v \\ p \end{pmatrix} = \begin{pmatrix} b_1 \\ b_2 \\ b_3 \end{pmatrix} \tag{7}$$

whose solution is:

$$\begin{pmatrix} u \\ v \\ p \end{pmatrix} = \begin{pmatrix} \dfrac{a_{23}a_{32}b_1 - a_{13}a_{32}b_2 + a_{13}a_{22}b_3}{a_{11}a_{23}a_{32} + a_{31}a_{13}a_{22}} \\ \dfrac{-a_{23}a_{31}b_1 + a_{13}a_{31}b_2 + a_{11}a_{23}b_3}{a_{11}a_{23}a_{32} + a_{31}a_{13}a_{22}} \\ \dfrac{a_{22}a_{31}b_1 + a_{11}a_{32}b_2 - a_{11}a_{22}b_3}{a_{11}a_{23}a_{32} + a_{31}a_{13}a_{22}} \end{pmatrix} \tag{8}$$

Having in mind the linear system (6) and its solution (7)-(8), the discretized system (6) may be rearranged in many different ways. The solution procedure presented in [2] re-writes Eq. (6) in all possible permutations of both velocity components adjacent to pressure (see [2] for full details).

The big advantage of this coupling procedure is that little memory is required to solve the corresponding linear system and that there are no errors in the boundary conditions. For the specific case of pressure, the problem is just an Initial Value Problem (IVP), and additionally in incompressible flows, only a reference for pressure is needed.

4 DISCRETIZATION PROCEDURE

The numerical procedure involves three different problems, the solution of the momentum, continuity and energy equation in the fluid:

$$\begin{gathered}\frac{\partial \vec{v}}{\partial t}+\rho(\vec{v}\cdot\nabla)\vec{v}=-\rho\vec{g}-\nabla p+\mu\nabla^2\vec{v}\\ \nabla\cdot\vec{v}=\vec{0}\\ \frac{\partial T}{\partial t}+(\vec{v}\cdot\nabla)T=\alpha\nabla^2\vec{v}\end{gathered} \tag{9}$$

In the solid, the only equation that has to be solved is the heat conduction:

$$\frac{\partial T}{\partial t}=\alpha\nabla^2\vec{v} \tag{10}$$

For the sake of simplicity, the general details of the discretization procedure are:

- Use a segregated grid arrangement for velocity components and pressure
- Locate the temperature in the same point as the pressure (fluid and solid)
- Discretize the diffusion term with second order finite differences
- Discretize the convection term with the Osher flux limiting scheme
- Use RBF to interpolate velocity components (needed in the flux limiting scheme)
- Use second order central differencing for pressure gradient
- Use second order central differencing for continuity equation
- Solve the resulting system (7) with the procedure explained in [2]

5 PROCEDURE FOR DIRECT NUMERICAL SIMULATION

5.1 Time integration scheme

The fundamental part of any DNS simulation is the right choice of the time integration scheme. Since the time scale for both (9) and (10) will be the same, the system of equations as a whole is a Differential Algebraic Equation, with some differential equations in time and others not (continuity).

Explicit schemes as Runge-Kutta and the classical predictor corrector Adams Bashford / Adams Moulton cannot be applied since there is way to compute the time derivative for pressure.

For this kind of differential systems, the only possible way is to use an implicit procedure. Here, the Adams Moulton is not suitable due to its limited stability region. Others such as Implicit Runge-Kutta (IRK) are hard to implement since their tableau is not diagonal dominant, fundamental condition for convergence of the linear system that has to be solved in each iteration.

The only suitable method is the so-called Backward-Differentiation Formulas (BDF) or implicit multistep, with a large stability region but computationally costly. Since in DNS, the inflow is going to be perturbed permanently (to produce turbulence), BDF of orders higher than 1 become unstable in certain cases and/or conditions and it is the procedure implemented here. Commercial packages such as Fluent, OpenFoam and Kiva report similar issues.

5.2 Inflow condition

The critical in any DNS simulation is the creation of perturbations in the inflow. The highly recommended *Precursor Simulation* has limited applicability because a periodic boundary condition must be implemented with the pseudo-spectral method as the only possible choice for solution, limited to cartesian coordinates only.

There are several other techniques used for the creation of inflow conditions but the main drawback is that a behavior is assumed in advance.

In order to avoid the inclusion of any predefined behavior, the white-noise technique will be used in this work. Since it is important to have perturbations with good statistical quality, the *Mersenne Twister* algorithm will be used [12]. This random number generator is very fast and it has a period of $2^{19,937}-1$, which is excellent for statistical studies.

The study of inflow perturbations on generation of turbulence will be performed with the following algorithm, trying to keep a strict control on the percentage of fluctuation. At any time step, the new inflow velocity will be computed by:

- Set an inflow velocity with the classical power profile to get a realistic boundary layer:

$$\frac{u_{Inflow}}{V_{Bulk}} = \left[1-|s|\right]^{1/100}; \quad -1 \le s \le +1 \tag{11}$$

- Select a set of random numbers (between -1 and +1) for every point in the inflow.
- Compute a *correction factor* f_x so the average of the fluctuations is 1:

$$f_x = \frac{A}{\int_A |x| dA} \tag{12}$$

- With p_f the *percentage of fluctuation*, compute the velocity fluctuation of each point:

$$v' = f_x p_f x v_{Inflow} \tag{13}$$

- Compute velocity correction δv to enforce mass continuity:

$$\delta v = V_{Bulk} - \frac{1}{A}\int_A \left(1 + f_x p_f x\right) v_{Inflow} dA \tag{14}$$

Finally, and in order to avoid high frequency oscillations, the inflow velocity already describes will be damped with respect to the previous time step, as used in other procedures such as OpenFoam.

5.3 Outflow condition

The outflow condition is also important to avoid the propagation of perturbations back to the flow. In this work, the convective outflow condition will be used:

$$\frac{\partial \phi}{\partial t} + V_n \frac{d\phi}{dn} = 0 \tag{15}$$

with V_n the average normal velocity of the corresponding outflow section and ϕ any scalar quantity, temperature and velocity components.

5.4 DNS parameters

The grid was built with 2 Kolmogorov deltas in the vertical direction and 12 Kolmogorov deltas in the direction of the flow for a Reynolds number of 5,000. The length of the expansion is 10 hydraulic diameters which is enough to hold completely the recirculation zone. The number of pressure points is about 166,000 for the expansion of 1.10 and over 200,000 for the expansion of 1.30. The delta time was small enough to keep the Courant number less than 1. At the inflow, a fluctuation factor of 20% was used and the damping factor was of 0.5.

6 BOUNDARY CONDITIONS

Additionally to the conditions for the DNS procedure itself, at the walls, no-slip condition is applied for velocity. As it was already explained, pressure needs no boundary conditions since is computed as an IVP, with one point fixed at a reference pressure.

For the thermal energy equation in the fluid, water at a dimensionless temperature of zero enters in the region and it is being heated by the step. The upper wall remains isolated and the lower wall that does not belong to the step remains isolated too.

The block, made of 304 carbon-steel has its left wall at a fixed dimensionless temperature of 1 degree and the lower wall remains isolated.

Finally, at the interphase that connects the block and the fluid, an energy balance is applied to compute the corresponding temperature:

$$-k_S \frac{dT^S}{dn} = -k_F \frac{dT^F}{dn} \tag{16}$$

Expressing the derivative of both fluid and solid, in terms of finite differences, the temperature of the interphase is:

$$T_i = \frac{-k_S \sum_{nb} a_{nb}^S T_{nb}^S - k_F \sum_{nb} a_{nb}^F T_{nb}^F}{k_S a_P^S + k_F a_P^F} \tag{17}$$

7 RESULTS AND DISCUSSION

Figure 1 shows the re-attachment length in terms for the expansion ratios of 1.1, 1.2 and 1.3 respectively. As expected, the reattachment is a linear function with a very small grow rate. This behavior is consistent with the experimental data published by Adams [13], in which a slight under prediction can be observed.

Figures 2 and 3 show the temperature distribution in the step. It is observed that as the aspect ratio increases, temperature gradients in the step become sharper due mainly to the increment in the recirculation of the flow.

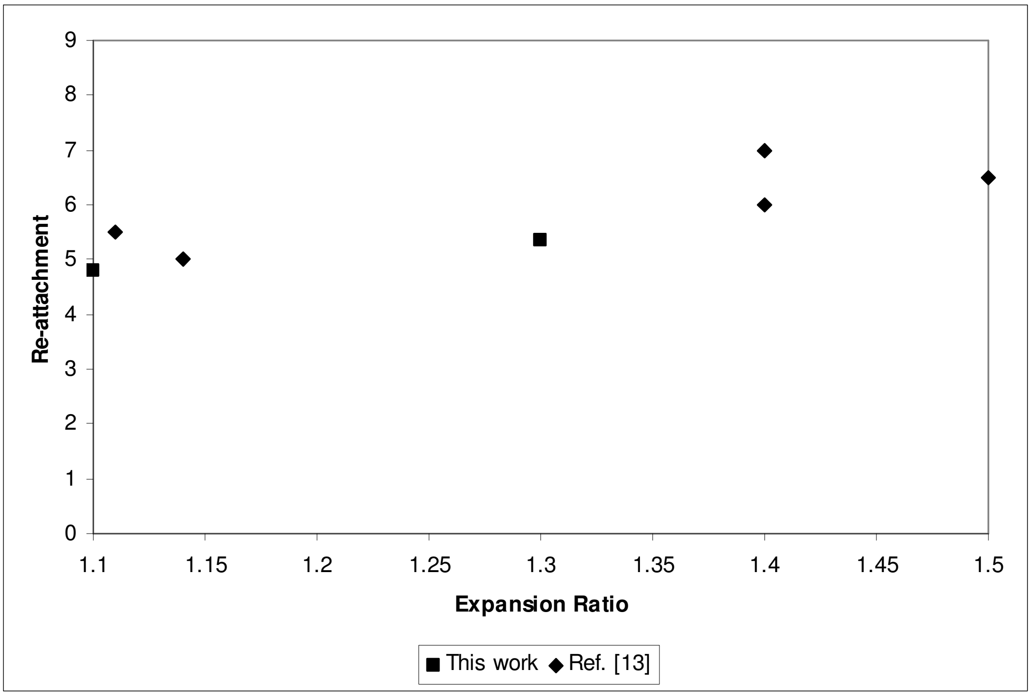

Figure 1: Re-attachment for different expansion ratios

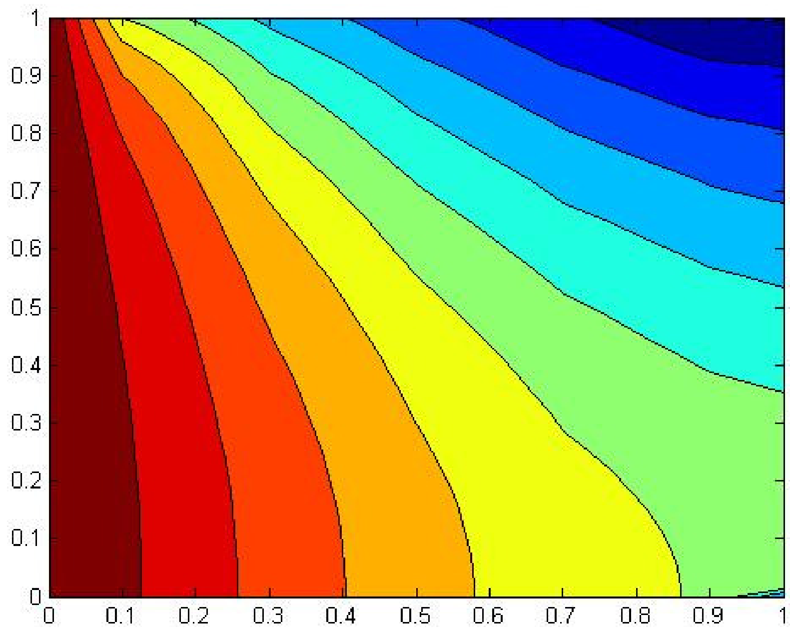

Figure 2: Temperature distribution in the step for an expansion ratio of 1.10

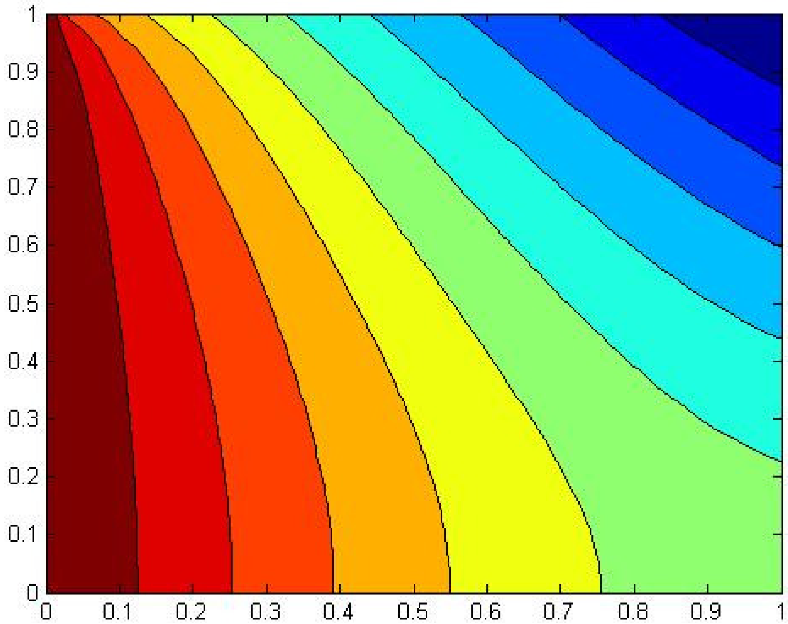

Figure 3: Temperature distribution in the step for an expansion ratio of 1.30

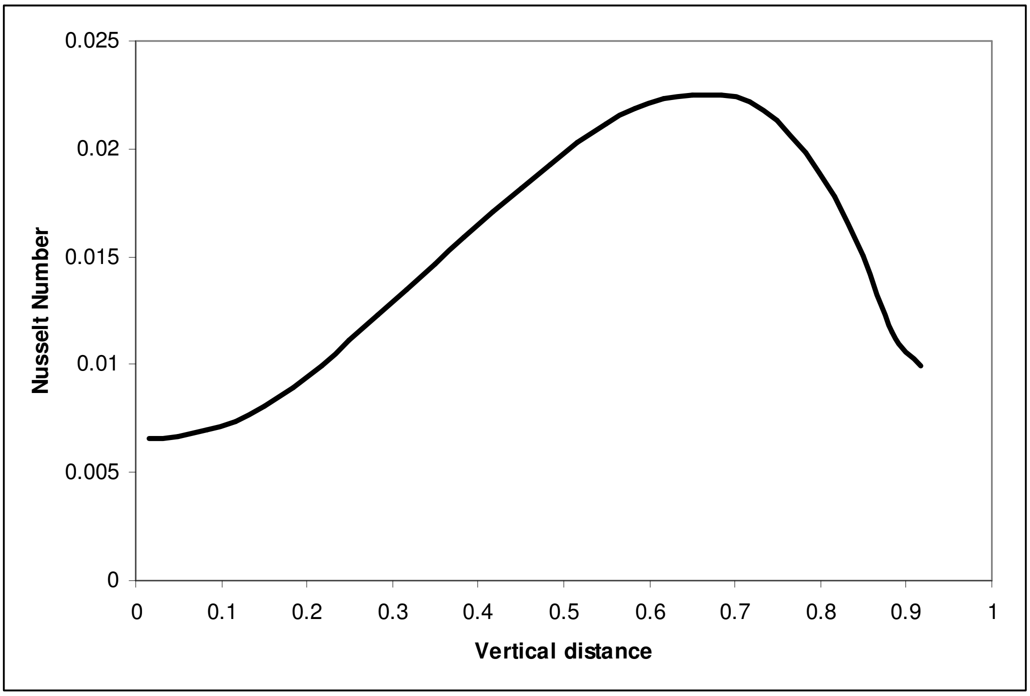

Figure 4: Nusselt number in the back wall for the expansion ratio of 1.10

Figure 4 shows the local Nusselt number in the back wall of the step. In the zone close to the lower wall, the gradient is small and becomes higher close to the corner (as expected). Even that there is no data to make a straight comparison, the shape and magnitude of the Nusselt number is consistent and in the same order of magnitude as it can be observed in references [3-10].

8 CONCLUSIONS

- A meshless procedure for DNS and LES simulations has been proposed.
- The re-attachment obtained for the expansion rations from 1.10 to 1.30 shows good agreement with experimental data.
- The behavior of the Nusselt number in the back wall is consistent with the one observed in previous publications.

REFERENCES

[1] Harlow, F. H. and Welch, F. E., *Numerical Calculation of Time-Dependent Viscous Incompressible Flow of Fluid with Free Surface*, Phys. Fluids (1965) **3:**2182-2189.

[2] Vidal, A. and Rodríguez, J., *A Direct Pressure-Linking Method for Turbulent Flow Computations*, Numer. Heat Transfer, Part B, (2007) **52**:531-549.

[3] Avancha, R. V. R. and Pletcher, R. H., *Large eddy simulation of the turbulent flow past a backward-facing step with heat transfer and property variations*, Int. J. Heat and Fluid Flow, (2002) **23**:601-614.

[4] Chen, Y. T., Nie, J. H., Armaly, B. F. and Hsieh H. T., *Turbulent separated convection flow adjacent to backward-facing step – effects on step height*, Int. J. Heat Mass Tran, (2006) **49**:3670-3680.

[5] Mushatet, K. S., *Simulation of Turbulent Flow and Heat Transfer over a Backward-Facing Step with Ribs Turbulators*, Thermal Science, (2011) **15**:245-255.

[6] Mushatet, K. S., *Study of Turbulent Flow and Heat Transfer Over a Backward-Facing Step Under Impingement Cooling*, Thi_Qar Univ. J. Eng. Sci., (2012) **3**:1-21.

[7] Pozarlik, A. K. and Kok, J. B. W., *Numerical Simulation of a Turbulent Flow Over a Backward Facing Step With Heated Wall: Effect of Pulsating Velocity and Oscillating Wall*, J. Therm. Sci. Eng. Appl., (2012) 4:041005.

[8] Rhee, G. H. and Sung H. J., *Enhancement of Heat Transfer in Turbulent Separated and Reattaching Flow by Local Forcing*, Numer. Heat Transfer, Part A, (2000) 37:733-753.

[9] Sakuraba, S., Fukazawa, K. and Sano, M., *Control of Turbulent Channel Flow over a Backward-Facing Step by Suction of Injection*, Heat Transfer – Asian Research, (2004) 33:490-504.

[10] Tsay, Y.-L., Chang, T. S., and Cheng, J. C., *Heat transfer enhancement of backward-facing step flow in a channel by using baffle installation on the channel flow*, Acta Mech., (2005) **174**:63-76.

[11] Patankar, S. V., *Numerical Heat Transfer and Fluid Flow*, Hemisphere (1980).

[12] Matsumoto, M., (2010), http://www.math.sci.hiroshima-u.ac.jp/~m-mat/MT/emt.html.

[13] Adams, E. W., Jhonston J. P., *Effects of the separating shear layer on the reattachment*

flow structure, Part 2: Reattachment length and wall shear stress, Exp. Fluids, (1988) **6**:493-499.